Effect of the substrate temperature on the synthesis of the Cu_2CoSnS_4 thin films by spray pyrolysis for solar cells devices

F. Harrathi[1,2], E. Aubry[3,4], S. Dridi[1,2], P. Briois[3], N. Bitri[1].

1 Laboratoire de Photovoltaïque et matériaux semi-conducteurs, Ecole Nationale d'Ingénieurs de Tunis, Université de Tunis El Manar, Tunis 1002, Tunisie

2 Ecole Nationale Supérieure d'Ingénieurs de Tunis, Université de Tunis, 5 Ave Taha Hussein, Tunis 1008, Tunisie

3 Institut FEMTO-ST, UMR 6174, CNRS, Université Bourgogne Franche-Comté, UTBM, Site de Montbéliard, 90010 Belfort, France

4 Institut FEMTO-ST, UMR 6174, CNRS, Université Bourgogne Franche-Comté, UFC, 2 Place Lucien Tharradin, Site de Montbéliard, 25200 Montbéliard, France

* Corresponding author: harrathifaouzia077@gmail.com

Abstract:

Cu_2CoSnS_4 (CCTS) thin films were directly prepared on glass substrates by chemical spray pyrolysis using distilled water as a solved agent under air ambiant. The X-ray diffraction analyses show that the CCTS thin films crystallize in stannite structure with a preferential orientation [112] from 280 to 360 °C. In addition, it is observed the crystallization of secondary phases mainly based on binary sulfides forming coarser nodules for all thin films. The surface morphology exhibits a granular, rough and compact topography. The magnitudes of the absorption coefficient for all the CCTS films are higher than 10^4 cm^{-1} in the visible range while the CCTS thin film deposited at 320 °C exhibits a band gap of 1.75 eV near than that those reported in the literature (~ 1.23-1.50 eV) and an electrical resistivity at room temperature of about 0.4 x 10^{-2} Ω.cm. Such optical and electrical properties suggest its use as an absorber layer in low cost solar cells.

Keywords: Cu_2CoSnS_4; thin films; spray pyrolysis; effect substrate temperature

1. Introduction

More than ever research into solar cells focused on a new generation to overcome the problems related to a sustainable production are essential. That is no longer based on silicone, but it uses

thin films which must be composed of non-toxic, abundant and cheap materials [1]. The quaternary family of chalcogenides Cu_2XSnS_4 (X = Ni, Zn, Co, Mn, Fe) has attracted a lot of attention as an absorber for applications in thin-film solar cell devices because of its excellent optical, electrical and chemical properties [2].

In this family, the Cu_2CoSnS_4 (CCTS) is relatively interested because its constituent elements are inexpensive, respectful of the environment and largely existing in nature [3]. In addition, the CCTS material has a p-type conductivity, a direct optical band gap of ~ 1.46–1.50 eV [4] and high absorption coefficient (> 10^4 cm^{-1}). Other properties like the thermoelectric of CCTS have been reported by different authors for different applications such as thermoelectric materials [5], photovoltaic [6], photocatalytic evolution of hydrogen [3], and electro-catalytic materials [7]. The CCTS materials were synthesized by various methods such as electrodeposition [8], solvothermal [9], electrospinning [3], or spin coating [10]. These methods require a liquid phase synthesis that needs a long heat treatment process followed by post-deposit steps such as washing, drying and calcination. These parameters lead to increase in production cost of the absorber layers [11]. Furthermore, there is another method consisting in the thin film synthesis by the spray pyrolysis technique. In addition, to enable the direct synthesis of sulfide films, the advantages of this technique compared to those mentioned above are its simplicity, its ability to treat large surfaces at a lower cost and it is environmentally friendly [12]. In addition, all of the copper-based quaternary semiconductors can be deposited by adjusting the spray deposition parameters such as film thickness [11], [13] substrate temperature [14], or the thiourea precursor concentration [15].

Amongst these parameters, the substrate temperature is the most optimized common parameter to obtain a quaternary thin film with desirable features [4], [14]. In the previous study of the impact of temperature on structural crystallization, methanol was used as solvent. In this study, CCTS thin films were prepared from distilled water as solvent agent instead of methanol which may cause troubles in large-scale use due to its toxicity. Then, the effect of substrate temperature on the formation of CCTS thin layers and their resulting properties such as the structure, chemical composition, optical and electrical properties is studied.

2. Material and methods

The CCTS thin films were deposited by spray pyrolysis on hot substrates under ambient atmosphere. The precursors $CuCl_2 \cdot 2H_2O$ (0.1 M) for copper, $CoCl_2 \cdot 6H_2O$ (0.1 M) for cobalt,

$SnCl_2 \cdot 2H_2O$ (0.1 M) for tin and NH_2CSNH_2 (0.1 M) for sulfur were dissolved in distilled water as the solvent agent and then mixed in a beaker under magnetic stirring for a few seconds.
The spraying solution was obtained by mixing 20 ml of $CuCl_2$, $CoCl_2$, $SnCl_2$ and 80 ml of thiourea to obtain the Cu:Co:Sn:S ratio as 2:1:1:16. It is noteworthy that the precursor was taked in the stoichiometric with the CCTS stoichiometry. However, thiourea was taked in excess to avoid sulfur loss during the spraying process on hot substrates.

The compressed air was utilized as carrier gas. In order to optimize the deposition temperature, the CCTS solution (100 mL) was sprayed onto a temperature range of 280–400 °C with an interval of 40 °C. Other deposition parameters of the spraying system such as the spray duration, the spray deposition rate, the gas flow rate, the distance nozzle-to-substrate and the hot plate rotation speed were set at: 30min, 3 × 10−3 L min-1, 10 L min-1, 20 cm, and 10 rpm, respectively. After deposition, the final samples were naturally cooled to room temperature.
Structural features of the coatings were investigated using X-ray diffraction (XRD, Bruker D8 Focus) with Co-$K_{\alpha 1+2}$ radiation ($\lambda = 1.78$ Å) operated in the scanning angle 2θ from 20 to 80° (Bragg-Brentano configuration, 0.02° step). Raman spectra were obtained by a Horiba Jobin Yvon T64000 spectrometer at room temperature under a 50 LF objective microscope, excited by a He-Ne laser. The surface morphology of the CCTS thin films was carried out by field emission scanning electron microscopy (FE-SEM JEOL JSM -7800 F). The cross-section observations were also carried out to estimate the thickness of the coating. The thicknesses of CCTS films deposited at different substrate temperatures such as 280, 320, 360, and 400 °C are 4.5, 1.2, 1.2, and 1 μm, respectively. The relatively large thickness of the film deposited at 280 °C is probably due to incomplete thermal decomposition of the spray droplets [16] [17] [18].
The chemical composition of the film deposited on glass substrates was estimated by energy dispersive spectroscopy (EDS Quantax Bruker with XFLASH 6|30 detector). The optical properties were determined by spectrophotometry (Shimadzu UV-3100S) with a spectral range 300-1800 nm and the results were visualized thanks to UV probe Spectrum hardware. Resistivity measurements were carried out on the CCTS film deposited on glass substrates at ambient temperature by the four-probe technique. The device is composed of a certified Jandel cell (Multi height probe, Jandel Engineering Limited), the factor shape is well known, and it is connected with an HP 3458A millimeter (Agilent) to measure electrical parameters.

- ❖ Formation mechanism of the CCTS thin films

The precursor solution for the formation of CCTS consists in the dissolution of the precursors in distilled water solvent according to these chemical equations [4]:

$$CuCl_2 \rightarrow Cu^{2+} + 2Cl^- \quad (1)$$

$$CoCl_2 \rightarrow Co^{2+} + 2Cl^- \quad (2)$$

$$SnCl_2 \rightarrow Sn^{2+} + 2Cl^- \quad (3)$$

$$SC(NH_2)_2 \rightarrow S^{2-} + H^+ + NH_2-C=NH \quad (4)$$

After spraying onto glass substrates, the formation of CCTS films under thermal decomposition can be explained by the following overall equation:

$$2CuCl_2 + CoCl_2 + SnCl_2 + 4CH_4N_2S + 10H_2O \rightarrow Cu_2CoSnS_4 + 8NH_4Cl\uparrow + 4CO_2\uparrow + 2H_2O\uparrow \quad (5)$$

3. Results and Discussion

3.1. Structural properties

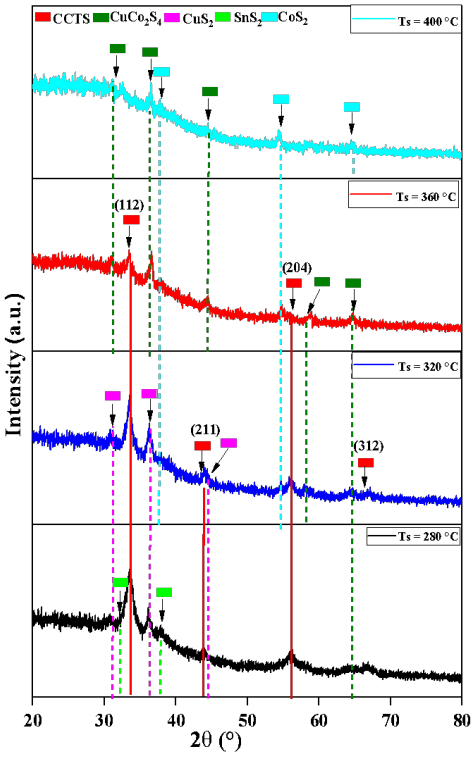

Figure. 1. *XRD diffractograms of CCTS thin films deposited at different substrate temperatures.*

Figure. 1 shows XRD patterns of CCTS thin films deposited at different substrate temperatures. Comparing the XRD patterns of CCTS thin films to a standard JCPDS Card00–026–0513, it is confirmed that the spray deposited CCTS thin films exhibit stannite tetragonal crystal structure (space group I-42m) with the preferential orientation [112] [19]. It is noteworthy that the increase of the substrate temperature leads to the X-ray intensity decrease to disappear at 400 °C. Since CCTS is a quaternary compound, second phase may form. The crystallization of the main structure comes with the formation of secondary phases based on sulfide such as villamaninite CuS_2 (space group Pa-3), cattierite CoS_2 (space group Pa-3), SnS_2 tin disulfide (space group P-3m1), and also carrollite $CuCo_2S_4$ ternary compound (space group Fd-3m) which its relative intensity increases with the deposition temperature. Below 360 °C, the main secondary phase is CuS_2, with traces of SnS_2, CoS_2 and $CuCo_2S_4$ phases, the SnS_2 phase being only detected at 280 °C. The relative X-ray intensity associated to the CuS_2 phase decreases progressively with the rise of the substrate temperature, unlike the X-ray intensities corresponding to the CoS_2 and $CuCo_2S_4$ which persists at elevated temperatures. At 360 °C, the main secondary phase becomes the ternary compound $CuCo_2S_4$ with traces of binary sulfides (CoS_2 and CuS_2). At the highest deposition temperature, i.e. 400 °C, only secondary phases ($CuCo_2S_4$ and CoS_2) crystallize. While the deposition was carried out under ambient atmosphere without any special precaution to avoid the film oxidation during the cooling, no oxides crystallization is clearly observed [12]. However, the CuO phase could be also confused with the CoS_2 compound at 54.4°, which the intensity peak increases with the temperature.

Furthermore, the crystallite size (D) considering spherical shape, the dislocation density (δ) and the microstrain (ε) were computed according to the below formulae [13]:

$$D = \frac{0.9\lambda}{\beta \cos\theta} \tag{6}$$

$$\delta = \frac{1}{D^2} \tag{7}$$

$$\varepsilon = \frac{\beta}{4\tan(\theta)} \tag{8}$$

Where β, θ, λ denote the experimental Full Width at the Half Maximum (FWHM in degree), the Bragg diffraction angle (°) and the X-ray wavelength (λ=*1.78* Å), respectively. It is

supposed that the instrumental contribution on the diffraction line width is negligible compared to that of induced by the crystallites and the micro strains. The calculated structural parameters are presented in the table.1.

Table.1. Structural parameters of the CCTS thin films deposited at different substrate temperatures.

Ts (°C)	FWHM (degree)	D (nm)	ε	δ (10^{-2} nm^{-2})
280	**1.29**	**7**	**1.6**	**1.7**
320	**0.85**	**11**	**0.7**	**0.7**
360	**0.50**	**19**	**0.4**	**0.2**

From table.1, it is observed that the crystallite size grows significantly from 7 to 19 nm with increasing substrate temperature. The similar trend of increase in crystallite size with respect to the temperature is observed in the synthesis of CCTS nanoparticles by thermal decomposition method [4]. In addition, the microstrains as well as the dislocation density observed in CCTS thin films decreases with the increase in substrate temperature from 280 to 360 °C. Therefore, the decrease of the microstrains and the dislocation density values could be considered as the decrease of the concentration of the mesh lattice imperfections with the deposition temperature rise. Besides, it can be observed that the increase of the substrate temperature leads to the decrease of the X-ray intensity of the main diffraction line of the CCTS phase. The deviation from the stoichiometry of the CCTS phase as well as the crystallization of secondary phases (as observed in 3.3) could disturb the crystallization of the CCTS phase by forming crystalline defects and/or amorphous CCTS phase [20].

Table.2. Structural parameters of the main secondary phases according to the substrate temperatures.

Ts (°C)	Nature of the main 2nd phase	Position (degree)	FWHM (degree)	D (nm)	δ (10^{-2} nm^{-2})
280	CuS_2	36.19	0.62	16	0.4
320	CuS_2	36.16	0.72	13	0.5
360	$CuCo_2S_4$	36.44	0.6	16	0.3
400	$CuCo_2S_4$	36.58	0.36	27	0.1

The table. 2, prove that the grain size of the CuS_2 decrease significantly from 16 nm to 13 nm when the temperature increases to Ts = 320 °C. At Ts = 360 °C, the secondary phases disappear and the $CuCo_2S_4$ appears with crystallite size of 27 nm.

3.2. Raman Characterization

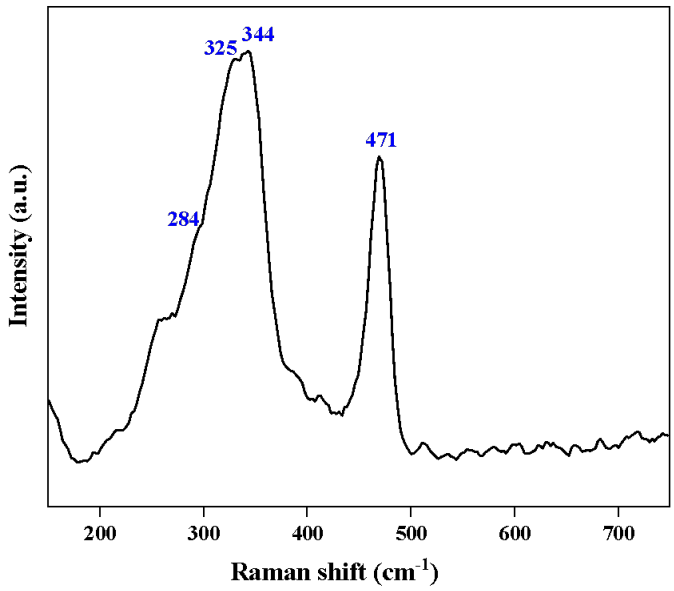

Figure.2. Raman spectra of CCTS thin film deposited at substrate temperature at 320 °C

To investigate the eventual presence and the nature of amorphous secondary phase, the Raman characterization technic being sensitive to short range spatial order has been applied to the thin

film synthesized at 320 °C, where the measurement was made at the wavelength range of 150–750 cm^{-1} (Figure.2).

The peaks located at 284, 325 and 344 cm^{-1} are clearly ascribed to the stannite structured Cu_2CoSnS_4 thin films, in agreement with the different studies [21], [22], [23], [24]. The peak located at 325 cm^{-1} corresponds to the symmetric vibrational motion of S atoms in the CCTS structure, whereas the peak at 284 cm^{-1} would be rather attributed to the vibrations of the Co and S atoms [6]. Besides, the sharp peak at 471 cm^{-1} with a high intensity could be assigned to the lattice vibration in copper sulfide compound (S-S vibrational stretching mode) which exhibits similar peak [25], [26], [27], [22], these results corroborate the XRD observations regarding the crystallization of secondary phases based on copper sulfide.

3.3. Chemical Composition

Table.3. Composition ratios of the CCTS thin films deposited at different substrate temperatures.

Ts (°C)	Cu/(Co+Sn)	Co/Sn	S/(Cu+Co+Sn)
280	**1.2**	**1.2**	**1**
320	**1.3**	**1.3**	**1**
360	**0.9**	**1.9**	**0.5**
400	**1.2**	**1.7**	**0.7**

To estimate the chemical composition of the thin films, EDS measurements has been implemented. For each film, several measurements have been done at different places, allowing the determination of the average concentration. Table.3 summarizes the compositional ratios of the constituent elements of CCTS films deposited at different substrate temperatures. As seen from the Table.3 the stoichiometry of the films deposited at 280 and 320 °C is relatively closed to that of the CCTS phase. The relatively slight excess in Cu could be at the origin of the CuS_2 compound formation. For films deposited at higher temperature, the deviation from the stoichiometry for the metallic elements increases with too high a Co content, which is consistent with the formation of $CuCo_2S_4$ compound. Furthermore, this effect is combined with a sulfide loss and film oxidation. Indeed, for films having a similar thickness, the O/Si chemical

composition ratio increases with the deposition temperature rise, witnessing of an oxidation phenomenon during the cooling. The disintegration and evaporation of some chemical entities inside the layers at high temperature, as shown by X. Zhang et al [28] could explain the deviation from the stoichiometry observed for the highest deposition temperature. Besides, the formation of binary sulfide such as CuS_2, CoS_2 or SnS_2 would also affect the stoichiometry of the Cu_2CoSnS_4 main phase.

3.4. Optical properties:

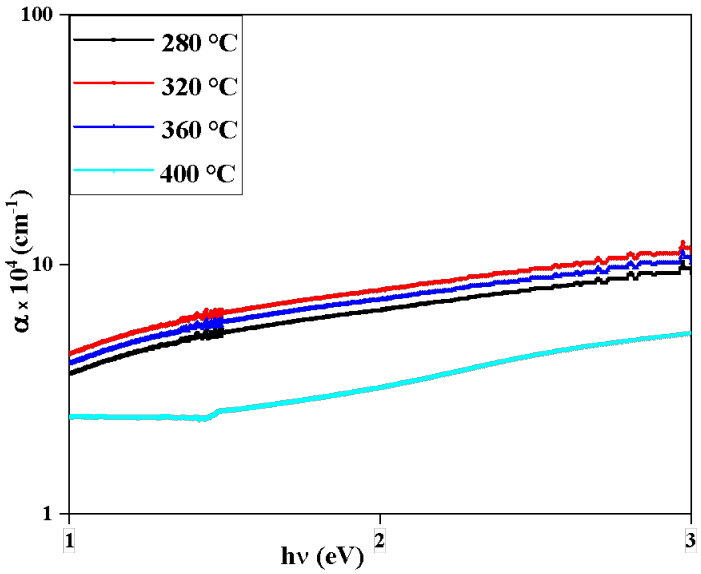

Figure.3. Variation of absorption coefficient (α) versus (hν) of CCTS films deposited at different substrate temperatures.

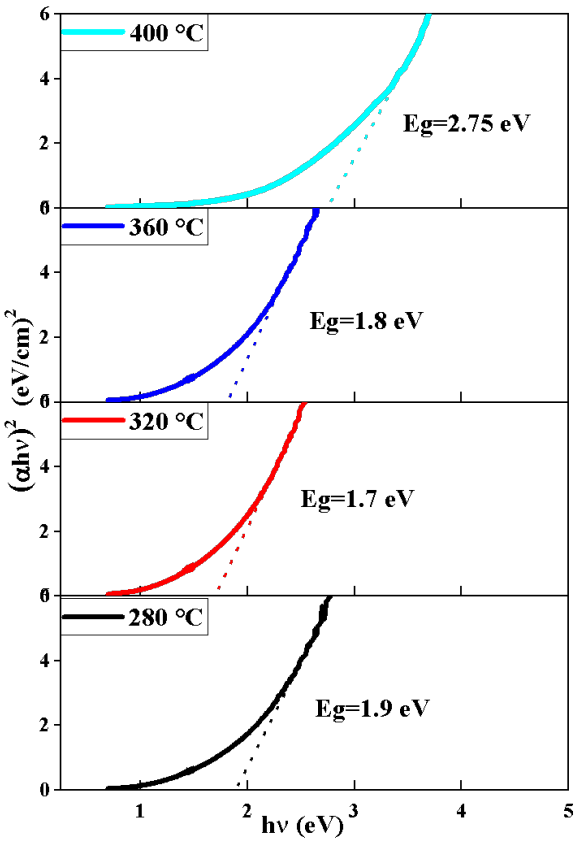

Figure.4. Variation of $(\alpha hv)^2$ versus (hv) of CCTS thin films deposited at different substrate temperatures.

The optical properties including the measurement of the absorption coefficient and band gap (Eg) of the CCTS thin films can be determined from these Tauc formulas [13]:

$$\alpha = \frac{1}{d} \times \ln\left(\frac{(1-R)^2}{T}\right) \tag{9}$$

$$\alpha hv = A(hv - Eg)^n \tag{10}$$

Where:

- hv: is the photon energy.
- Eg: is the optical band gap.
- α: is the absorption coefficient.
- A: is the proportionality constant.

- $\underline{n}$: is a constant taking value equal to ½ for direct bandgap.

The evolutions of the absorption coefficient (α) as a function of photon energy (hν) of CCTS films deposited at different substrate temperatures are shown in Fig. 3. It can be seen that the absorption coefficient of all films in the visible range are greater than 10^4 cm^{-1}. However, the absorption coefficient of films deposited at 400 °C dropped sharply but remained high in the visible range. The non-crystallization of the CCTS phase or the relatively close stoichiometry deviation observed at 360 and 400 °C cannot explain this difference, and an oxidation of the coating would rather be responsible. These high absorption coefficients are consistent with other reports [12] and are considered suitable absorber layers in thin-film solar cells.

The band gap energies of the films were determined by extrapolating the linear portion of the plots to the photon energies axis considering direct transition (see Fig. 4). However, these values are slightly higher than that those reported in literature (Eg ~ 1.23-1.45 eV) [4]. The formation of secondary phases based on sulfide compound with higher band gap values than that of the CCTS phase would explain the higher observed band gap energy range (CuS_2 1.87 eV [29], $CuCo_2S_4$ 0.43 eV [30], 2.15 eV 2.24 eV [31], CoS_2 2.2 eV [32] , SnS_2 2.22 eV [33]. In addition, the oxidation of the films combined with the sulfide loss for films deposited at high temperature would favor the formation of amorphous oxides having higher optical bandgap (1.3-2.1 eV for CuO [34], 3.65 eV for $CuCoO_2$ [35]) resulting in the increase of the optical bandgap of the film deposited at 400 °C. Furthermore, the fluctuate in band gap energies with increase substrate temperature could also arise from the stimulus of various factors, including the crystalline size observed from XRD pattern, presence of impurities, and deviation from stoichiometry [36].

3.5. Morphological Characterization

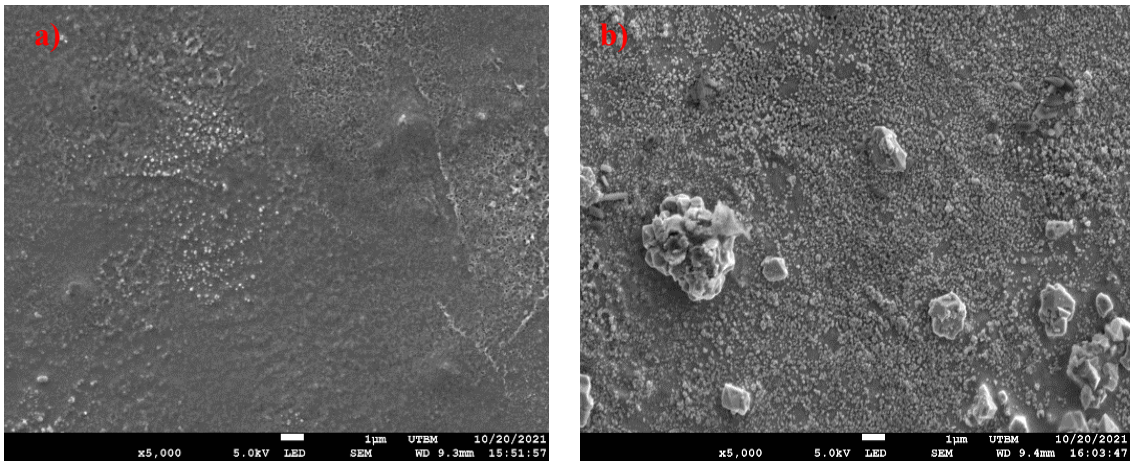

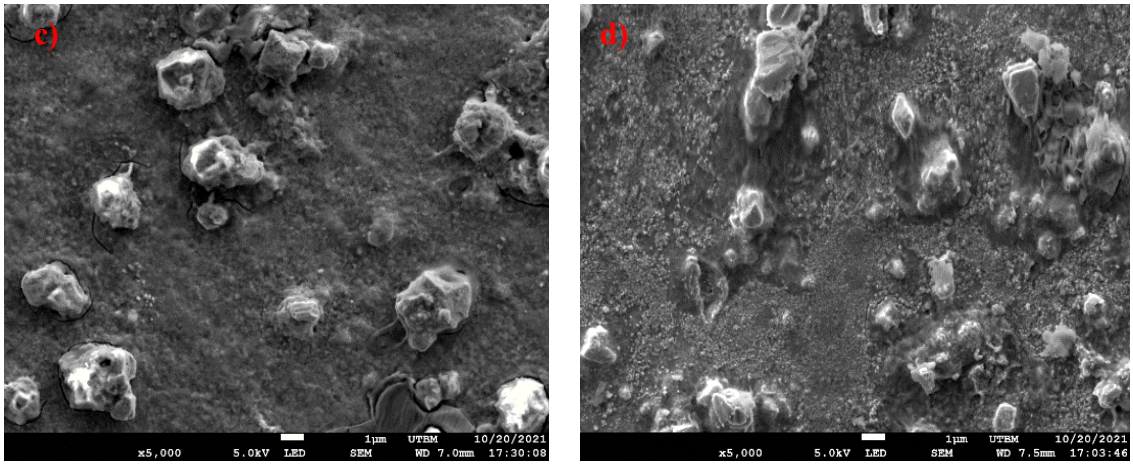

Figure.5. Surface SEM images of CCTS thin films synthesized at different substrate temperatures: a) T_s = 280 °C, b) T_s = 320 °C, c) T_s =360 °C, d) T_s = 400 °C.

The morphological features of CCTS-based thin films deposited on glass substrates at different substrate temperatures are assessed with scanning electron microscopy (see Figure.5). The surface of CCTS thin film prepared at 280 °C is found to be uniform, rough and compact. No voids nor cracks are observed throughout the whole glass substrate, only fine nodules constitute the surface. With a further increase of the substrate temperature, coarser nodules are formed in addition to the uniform and compact surface of CCTS thin film. X-ray energy dispersive spectroscopy measurements on the coarser nodules (see Fig. 6) demonstrate that they are mainly constituted of Cu and S in agreement with our previous observations with XRD and Raman spectroscopy. In reason of the interaction volume being to large regarding the size of the nodules, the stoichiometry cannot be estimated. Others measures in different nodules have also shown a slight enrichment in Co and S, or in Co, Cu and S confirming traces of CoS_2 and $CuCo_2S_4$ in films deposited at 320 °C.

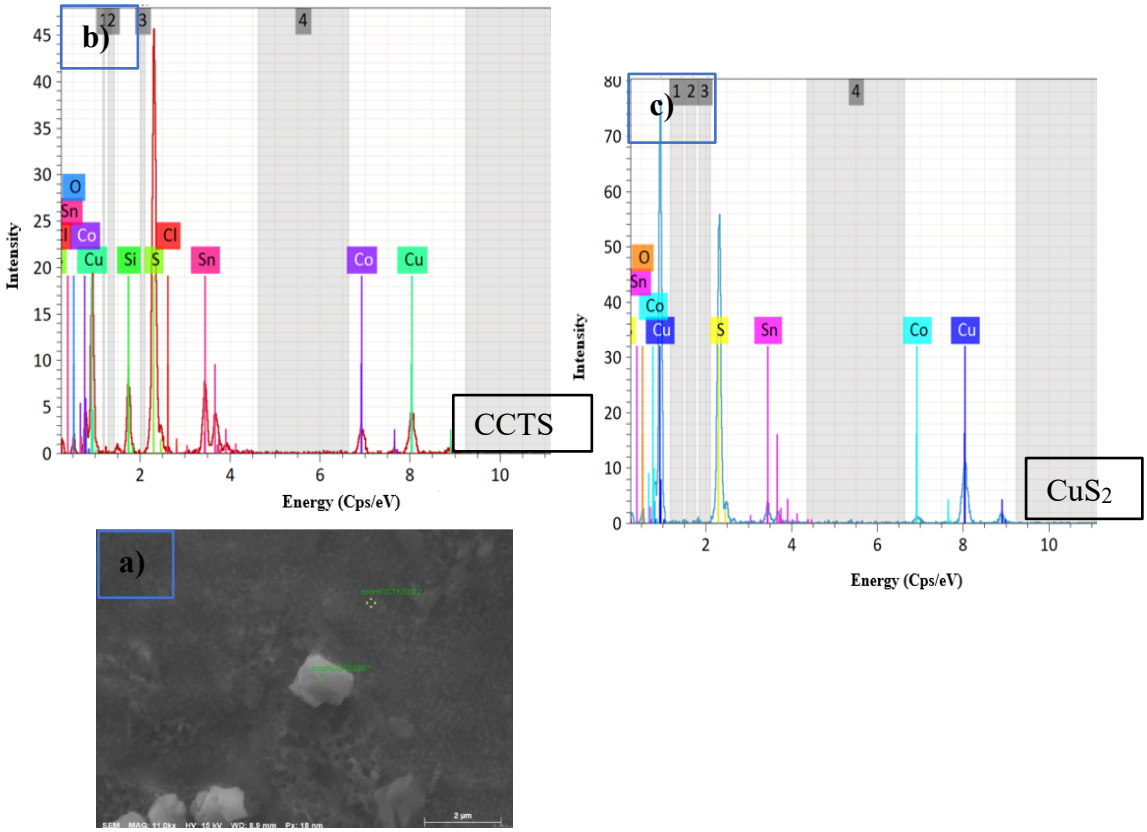

Figure.6. a) Surface of the CCTS thin film deposited at substrate temperature at 320 °C b) with corresponding EDS spectra of CCTS thin film c) and nodule based on copper sulfide

3.6. Electrical properties

Table.4. Electrical resistivity of the CCTS thin films deposited at different substrate temperatures:

Temperature (°C)	**Sheet resistance (Ω/sq)**	**Electrical resistivity (x 10^{-2} Ω·cm)**
280	**8**	**2**
320	**41**	**0.4**
360	**64**	**3.7**
400	**69**	**3.4**

The electrical resistivity of CCTS thin films at room temperature was measured by the four-probe method. As shown in the table.4 the electrical resistivity of all CCTS thin films varies between 0.43 x 10^{-2} and 3.70 x 10^{-2} Ω.cm. The electrical resistivity of CCTS thin films decreases by twice order of magnitude compared with that obtained in Cu_2MnSnS_4 spray deposited film [12], and is also the same order of magnitude with CIGS films [37]. The relative improvement of the electrical conductivity with a further increase of the deposition temperature from 280 to 320 °C would be ascribed, in 1st approximation, to the coarser grain size and to the lower dislocation density and microstrain values of the CCTS phase resulting in a lower charge carrier diffusion. However, it is noteworthy that the films deposited at 360 and 400 °C exhibit a slightly higher electrical resistivity values, despite a favorable decrease of the grain size and dislocation density in CCTS and also the appearance of copper oxides (CuO has a very low conductivity value and consequently a greater resistivity). The stoichiometry deviation of the films deposited at the highest temperatures (excess of Co, loss of sulfur, and oxygen enrichment), combined with the crystallization of the secondary phases only at 400 °C such as cobalt sulfide (~1.7 × 10^6 Ω.cm [38]) or highly resistive copper oxide (> 10^4 Ω.cm [39]), prevail on the positive effect of CCTS crystallinity improvement with the rise of the elevation temperature [40]. However, the electrical resistivity of films deposited at 400 °C is unexpectedly slightly lower than that of synthesized at 360 °C. This phenomenon could arise from the relative high electrical conductivity of the $CuCo_2S_4$ compound since it is subject of intensive research in electrochemical capacitors and thermoelectric materials [41][42].

4. Conclusions

The CCTS thin films have been deposited using spray pyrolysis method in using distilled water as solvent agent at different substrate temperatures (T_s = 280, 320, 360 and 400 °C). Structural results prove that the films synthesized with a substrate temperature less than 400 °C crystallize in stannite structure, with the crystallization of secondary phases mainly based on binary sulfides forming coarser nodules. It was shown that the rise of the deposition temperature leads to the grain size increase with a diminution of the dislocation density and microstrains. However, the stoichiometry deviation in the CCTS film increases with the temperature: Co excess and sulfur loss at moderate deposition temperature, then oxidation at higher temperature. The absorption coefficient has been found higher than 10^4 cm^{-1} in the visible range with an estimated band gap value slightly higher to its theoretical value. The electrical results prove that

the CCTS film exhibits an electrical resistivity corresponding to other quaternary sulfides. The general improvement in physical properties obtained for the CCTS thin film deposited at T_s = 320 °C would be the result of a minimal stoichiometry deviation while managing to improve the crystallinity of the CCTS phase. Analysis of these experimental results confirms that 320 °C is the optimum substrate temperature, which making CCTS thin film a promising absorbent material in low cost solar cell devices. The performance of the CCTS thin film by spray pyrolysis in using distilled water as solvent agent instead of toxic methanol are competitive with the standard properties of CCTS films.

Author Contributions: F.H Investigation, Writing - original draft, Visualization.

E.A: Data curation, formal analysis- editing, and software.

S.D: formal analysis.

N.B and P.B. supervision-resources- project administration.

Data availability: Data sharing is not relevant to this article as no dataset was generated or analyzed during the current study.

Declaration of Competing Interest: The authors declare no conflicts of interest.

Declaration of ethical approval: The authors declare that this article does not contain any human intervention research conducted by any of the authors. Results are well placed in the context of previous and existing studies

Acknowledgments: authors wish to acknowledge the Tunisian Ministry of Higher Education and Scientific Research for financial support of this work. This work was done within the FEMTO-ST SURFACE platform.

References

[1] I. Bargaoui, N. Bitri, S. Dridi, and I. Ly, 'Cu2CoSnS4 thin films as suitable absorber layers for photovoltaic applications, synthesized by spray pyrolysis, *Mater. Res. Express*, vol. 6, no. 8, p. 086410, 2019.

[2] S. Dridi, N. Bitri, and M. Abaab, 'Synthesis of quaternary Cu2NiSnS4 thin films as a solar energy material prepared through «Spray» technique', *Mater. Lett.*, vol. 204, pp. 61–64, 2017.

[3] F. Ozel, E. Aslan, B. Istanbullu, O. Akay, and I. H. Patir, 'Photocatalytic hydrogen evolution based on Cu2ZnSnS4, Cu2NiSnS4 and Cu2CoSnS4 nanocrystals', *Appl. Catal. B Environ.*, vol. 198, pp. 67–73, 2016.

[4] P. S. Maldar *et al.*, 'Fabrication of Cu2CoSnS4 thin films by a facile spray pyrolysis for photovoltaic application', *Sol. Energy*, vol. 158, pp. 89–99, 2017.

[5] D. Zhang *et al.*, ‘Multi-cations compound Cu2CoSnS4: DFT calculating, band engineering and thermoelectric performance regulation’, *Nano Energy*, vol. 36, pp. 156–165, 2017.
[6] M. Krishnaiah, P. Bhargava, and S. Mallick, ‘Low-temperature synthesis of Cu 2 CoSnS 4 nanoparticles by thermal decomposition of metal precursors and the study of its structural, optical and electrical properties for photovoltaic applications’, *RSC Adv.*, vol. 5, no. 117, pp. 96928–96933, 2015.
[7] K. Mokurala, S. Mallick, and P. Bhargava, ‘Alternative quaternary chalcopyrite sulfides (Cu2FeSnS4 and Cu2CoSnS4) as electrocatalyst materials for counter electrodes in dye-sensitized solar cells’, *J. Power Sources*, vol. 305, pp. 134–143, 2016.
[8] J. Yu *et al.*, ‘Synthesis of Cu2MnSnS4 thin film deposited on seeded fluorine doped tin oxide substrate via a green and low-cost electrodeposition method’, *Mater. Lett.*, vol. 191, pp. 186–188, 2017.
[9] Y. Cui, R. Deng, G. Wang, and D. Pan, ‘A general strategy for synthesis of quaternary semiconductor Cu 2 MSnS 4 (M= Co 2+, Fe 2+, Ni 2+, Mn 2+) nanocrystals’, *J. Mater. Chem.*, vol. 22, no. 43, pp. 23136–23140, 2012.
[10] A. Ghosh, A. Biswas, R. Thangavel, and G. Udayabhanu, ‘Photo-electrochemical properties and electronic band structure of kesterite copper chalcogenide Cu 2–II–Sn–S 4 (II= Fe, Co, Ni) thin films’, *RSC Adv.*, vol. 6, no. 98, pp. 96025–96034, 2016.
[11] P. S. Maldar, A. A. Mane, S. S. Nikam, S. D. Dhas, and A. V. Moholkar, ‘Spray deposited Cu2CoSnS4 thin films for photovoltaic application: Effect of film thickness’, *Thin Solid Films*, vol. 709, p. 138236, 2020.
[12] S. Dridi, E. Aubry, N. Bitri, F. Chaabouni, and P. Briois, ‘Growth and Characterization of Cu2MnSnS4 Thin Films Synthesized by Spray Pyrolysis under Air Atmosphere’, *Coatings*, vol. 10, no. 10, p. 963, 2020.
[13] H. Y. S. Al-Zahrani, ‘Synthesis, optical and optoelectrical analysis of the Cu2CoSnS4 thin films as absorber layer for thin-film solar cells’, *J. Mater. Sci. Mater. Electron.*, vol. 31, no. 9, pp. 6900–6909, 2020.
[14] C. Nefzi, M. Souli, Y. Cuminal, and N. Kamoun-Turki, ‘Effect of substrate temperature on physical properties of Cu2FeSnS4 thin films for photocatalysis applications’, *Mater. Sci. Eng. B*, vol. 254, p. 114509, 2020.
[15] M. A. Ahmed, N. A. Bakr, and A. A. Kamil, ‘Synthesis and characterization of chemically sprayed Cu2CoSnS4 Thin Films’, *Chalcogenide Lett.*, vol. 16, no. 5, pp. 231–239, 2019.
[16] P. S. Maldar, A. A. Mane, S. S. Nikam, S. D. Giri, A. Sarkar, and A. V. Moholkar, ‘Temperature dependent properties of spray deposited Cu2CoSnS4 (CCTS) thin films’, *J. Mater. Sci. Mater. Electron.*, vol. 28, no. 24, pp. 18891–18896, Dec. 2017, doi: 10.1007/s10854-017-7842-1.
[17] M. Krunks, O. Bijakina, T. Varema, V. Mikli, and E. Mellikov, ‘Structural and optical properties of sprayed CuInS2 films’, *Thin Solid Films*, vol. 338, no. 1–2, pp. 125–130, Jan. 1999, doi: 10.1016/S0040-6090(98)01069-4.
[18] A. A. Mane and A. V. Moholkar, ‘Orthorhombic MoO3 nanobelts based NO2 gas sensor’, *Appl. Surf. Sci.*, vol. 405, pp. 427–440, May 2017, doi: 10.1016/j.apsusc.2017.02.055.
[19] M. Krishnaiah, R. K. Mishra, S. G. Seo, S. H. Jin, and J. T. Park, ‘Highly crystalline, large grain Cu2CoSnS4 films with reproducible stoichiometry via direct solution spin coating for optoelectronic device application’, *Ceram. Int.*, vol. 45, no. 9, pp. 12399–12405, 2019.
[20] J. L. van Heerden and R. Swanepoel, ‘XRD analysis of ZnO thin films prepared by spray pyrolysis’, *Thin Solid Films*, vol. 299, no. 1–2, pp. 72–77, May 1997, doi: 10.1016/S0040-6090(96)09281-4.

[21] C. Nefzi, M. Souli, J. L. Costa-Krämer, J. M. García, and N. Kamoun-Turki, 'Growth of the next generation promising Cu2 Fe1-xCoxSnS4 thin films and efficient p-CCTS/n-In2S3/n-SnO2F heterojunction for optoelectronic applications', *Mater. Res. Bull.*, vol. 133, p. 111028, Jan. 2021, doi: 10.1016/j.materresbull.2020.111028.
[22] M. Oubakalla *et al.*, 'Effects of copper concentration on the properties of Cu2CoSnS4 thin films co-electrodeposited on the FTO substrate', *J. Mater. Sci. Mater. Electron.*, vol. 33, no. 15, pp. 12016–12025, 2022.
[23] M. K. Sahoo, M. Gusain, S. Thangriyal, R. Nagarajan, and G. R. Rao, 'Energy storage study of trimetallic Cu2MSnS4 (M: Fe, Co, Ni) nanomaterials prepared by sequential crystallization method', *J. Solid State Chem.*, vol. 282, p. 121049, Feb. 2020, doi: 10.1016/j.jssc.2019.121049.
[24] M. Beraich *et al.*, 'Synthesis and characterization of Cu2CoSnS4 thin film via electrodeposition technique for solar cells', *J. Mater. Sci. Mater. Electron.*, vol. 30, no. 13, pp. 12487–12492, Jul. 2019, doi: 10.1007/s10854-019-01608-2.
[25] M. Ishii, K. Shibata, and H. Nozaki, 'Anion Distributions and Phase Transitions in CuS1-xSex(x = 0-1) Studied by Raman Spectroscopy', *J. Solid State Chem.*, vol. 105, no. 2, pp. 504–511, Aug. 1993, doi: 10.1006/jssc.1993.1242.
[26] T. Hurma and S. Kose, 'XRD Raman analysis and optical properties of CuS nanostructured film', *Optik*, vol. 127, no. 15, pp. 6000–6006, Aug. 2016, doi: 10.1016/j.ijleo.2016.04.019.
[27] M. Beraich *et al.*, 'Preparation and characterization of Cu2CoSnS4 thin films for solar cells via co-electrodeposition technique: Effect of electrodeposition time', *Optik*, vol. 193, p. 162996, Sep. 2019, doi: 10.1016/j.ijleo.2019.162996.
[28] X. Zhang, N. Bao, B. Lin, and A. Gupta, 'Colloidal synthesis of wurtzite Cu2CoSnS4 nanocrystals and the photoresponse of spray-deposited thin films', *Nanotechnology*, vol. 24, no. 10, p. 105706, 2013.
[29] N. Bouguila *et al.*, 'Investigation of some physical and photoconductive properties of sprayed CuS2 film', *J. Mater. Sci. Mater. Electron.*, vol. 33, no. 7, pp. 3810–3821, Mar. 2022, doi: 10.1007/s10854-021-07572-0.
[30] N. Sethulakshmi *et al.*, 'Nanocoral CuCo2S4 thiospinels: Oxygen evolution reaction via redox interaction of metal ions', *Electrochimica Acta*, vol. 370, p. 137701, Feb. 2021, doi: 10.1016/j.electacta.2020.137701.
[31] M. Chauhan, K. Soni, P. E. Karthik, K. P. Reddy, C. S. Gopinath, and S. Deka, 'Promising visible-light driven hydrogen production from water on a highly efficient $CuCo_2S_4$ nanosheet photocatalyst', *J. Mater. Chem. A*, vol. 7, no. 12, pp. 6985–6994, 2019, doi: 10.1039/C9TA00391F.
[32] X. Ma *et al.*, 'Three narrow band-gap semiconductors modified Z-scheme photocatalysts, Er3+:Y3Al5O12@NiGa2O4/(NiS, CoS2 or MoS2)/Bi2Sn2O7, for enhanced solar-light photocatalytic conversions of nitrite and sulfite', *J. Ind. Eng. Chem.*, vol. 66, pp. 141–157, Oct. 2018, doi: 10.1016/j.jiec.2018.05.024.
[33] N. G. Deshpande, A. A. Sagade, Y. G. Gudage, C. D. Lokhande, and R. Sharma, 'Growth and characterization of tin disulfide (SnS2) thin film deposited by successive ionic layer adsorption and reaction (SILAR) technique', *J. Alloys Compd.*, vol. 436, no. 1–2, pp. 421–426, Jun. 2007, doi: 10.1016/j.jallcom.2006.12.108.
[34] H. Zare Asl and S. Mohammad Rozati, 'Spray deposited nanostructured CuO thin films: influence of substrate temperature and annealing process', *Mater. Res.*, vol. 21, 2018.
[35] H. Widjaja *et al.*, 'DFT + U and ab initio atomistic thermodynamics approache for mixed transitional metallic oxides: A case study of CoCu 2 O 3 surface terminations', *Mater. Chem. Phys.*, vol. 201, pp. 241–250, Nov. 2017, doi: 10.1016/j.matchemphys.2017.08.047.

[36] S. G. Nilange, N. M. Patil, and A. A. Yadav, 'Influence of precursor thiourea contents on the properties of spray deposited Cu2FeSnS4 thin films', *Phys. B Condens. Matter*, vol. 570, pp. 73–81, 2019.
[37] F. Mesa, C. Calderón, and G. Gordillo, 'Study of electrical properties of CIGS thin films prepared by multistage processes', Thin Solid Films, vol. 518, no. 7, pp. 1764–1766, Jan. 2010, doi: 10.1016/j.tsf.2009.09.028.
[38] T. Abza et al., 'Characterization of Cobalt Sulfide Thin Films Synthesized from Acidic Chemical Baths', Adv. Mater. Sci. Eng., vol. 2020, pp. 1–9, Apr. 2020, doi: 10.1155/2020/2628706.
[39] L. De Los Santos Valladares et al., 'Crystallization and electrical resistivity of Cu2O and CuO obtained by thermal oxidation of Cu thin films on SiO2/Si substrates', Thin Solid Films, vol. 520, no. 20, pp. 6368–6374, Aug. 2012, doi: 10.1016/j.tsf.2012.06.043.
[40] A.-S. Gadallah, M. A. Salim, T. Atwee, and A. M. Ghander, 'Effect of Al doping on structural, morphological, optical, and electrical properties of Cu2ZnSnS4 thin films prepared by sol-gel spin coating', Optik, vol. 159, pp. 275–282, 2018.
[41] Y. Lang, L. Pan, C. Chen, and Y. Wang, 'Thermoelectric Properties of Thiospinel-Type CuCo2S4', J. Electron. Mater., vol. 48, no. 7, pp. 4179–4187, Jul. 2019, doi: 10.1007/s11664-019-07182-x.
[42] J.-M. Xu, X.-C. Wang, and J.-P. Cheng, 'Supercapacitive Performances of Ternary CuCo 2 S 4 Sulfides', ACS Omega, vol. 5, no. 3, pp. 1305–1311, Jan. 2020, doi: 10.1021/acsomega.9b03865.